

## Dose conversion coefficients for photon exposure of the human eye lens

This content has been downloaded from IOPscience. Please scroll down to see the full text.

2011 Phys. Med. Biol. 56 415

(<http://iopscience.iop.org/0031-9155/56/2/009>)

View [the table of contents for this issue](#), or go to the [journal homepage](#) for more

Download details:

IP Address: 193.136.74.116

This content was downloaded on 29/05/2017 at 14:52

Please note that [terms and conditions apply](#).

You may also be interested in:

[Dose conversion coefficients for electron exposure of the human eye lens](#)

R Behrens, G Dietze and M Zankl

[Dose conversion coefficients for monoenergetic electrons incident on a realistic human eye model](#)

P Nogueira, M Zankl, H Schlattl et al.

[On the operational quantity  \$H\_p\(3\)\$  for eye lens dosimetry](#)

R Behrens

[Organ dose conversion coefficients for reference adult male and female](#)

H Schlattl, M Zankl and N Petoussi-Henss

[Organ dose conversion coefficients on an ICRP-based CAM voxel model](#)

Liye Liu, Zhi Zeng, Junli Li et al.

[An ICRP-based Chinese adult male voxel model and its absorbed dose for idealized photon exposures](#)

Liye Liu, Zhi Zeng, Junli Li et al.

[On the feasibility of utilizing active personal dosimeters worn on the chest to estimate occupational eye lens dose in x-ray angiography](#)

Artur Omar, Maria Marteinsdottir, Nils Kadesjö et al.

[Voxel model organ doses for external photon irradiation](#)

M Zankl, U Fill, N Petoussi-Henss et al.

# Dose conversion coefficients for photon exposure of the human eye lens

R Behrens<sup>1</sup> and G Dietze<sup>2</sup>

<sup>1</sup> Physikalisch-Technische Bundesanstalt, Bundesallee 100, D-38116 Braunschweig, Germany

<sup>2</sup> Paracelsusstraße 7, D-38116 Braunschweig, Germany

E-mail: [rolf.behrens@ptb.de](mailto:rolf.behrens@ptb.de)

Received 3 September 2010, in final form 22 November 2010

Published 22 December 2010

Online at [stacks.iop.org/PMB/56/415](http://stacks.iop.org/PMB/56/415)

## Abstract

In recent years, several papers dealing with the eye lens dose have been published, because epidemiological studies implied that the induction of cataracts occurs even at eye lens doses of less than 500 mGy. Different questions were addressed: Which personal dose equivalent quantity is appropriate for monitoring the dose to the eye lens? Is a new definition of the dose quantity  $H_p(3)$  based on a cylinder phantom to represent the human head necessary? Are current conversion coefficients from fluence to equivalent dose to the lens sufficiently accurate? To investigate the latter question, a realistic model of the eye including the inner structure of the lens was developed. Using this eye model, conversion coefficients for electrons have already been presented. In this paper, the same eye model—with the addition of the whole body—was used to calculate conversion coefficients from fluence (and air kerma) to equivalent dose to the lens for photon radiation from 5 keV to 10 MeV. Compared to the values adopted in 1996 by the International Commission on Radiological Protection (ICRP), the new values are similar between 40 keV and 1 MeV and lower by up to a factor of 5 and 7 for photon energies at about 10 keV and 10 MeV, respectively. Above 1 MeV, the new values (calculated without kerma approximation) should be applied in pure photon radiation fields, while the values adopted by the ICRP in 1996 (calculated with kerma approximation) should be applied in case a significant contribution from secondary electrons originating outside the body is present.

(Some figures in this article are in colour only in the electronic version)

## 1. Introduction

The lens of the human eye is sensitive to exposure by ionizing radiation mainly due to the induction of a cataract in the lens. In the past, the cataract has been seen as a deterministic

effect with a threshold of more than about 0.5 Gy at minimum, see table A.3.1 in ICRP Publication 103 (ICRP 2007). ICRP has, therefore, defined a specific annual dose limit for the lens of the eye of 150 mSv for occupationally exposed persons and 15 mSv for members of the public. On the other hand, ICRP stated in paragraph A 80 of ICRP 103 that it cannot ultimately be excluded that a cataract can be induced at even lower doses, which is supported by recent epidemiological studies (Worgul *et al* 2007, Chodick *et al* 2008). Therefore, several questions are currently being discussed: Which personal dose equivalent quantity is appropriate for monitoring the exposure of the eye lens? (Behrens and Dietze 2010). Is a new definition of the personal dose quantity,  $H_p(3)$ , based on a cylinder phantom representing the human head necessary? (Daures *et al* 2009, Mariotti and Gualdrini 2009).

In order to discuss which dose quantity is suitable to monitor the exposure of the eye lens, the real dose produced has to be determined. Doses in the eye lens are not measurable and hence conversion coefficients are generally used which are achieved by Monte Carlo calculations, where the eye and the body are simulated and irradiated by monoenergetic radiation, and conversion coefficients from fluence or air kerma to equivalent dose are calculated:  $H_T/\Phi$  and  $H_T/K_a$  for electrons and photons, respectively, with  $H_T$  the equivalent dose to the eye lens,  $K_a$  the air kerma, and  $\Phi$  the incident particle fluence. Values for photons and electrons were published in ICRP Publication 74 (ICRP 1996). These data were calculated using the geometrically defined ADAM phantom (Kramer *et al* 1982) which does not describe the geometry of the eye in detail. In a recent work, a more realistic model of the eye was applied in order to obtain more reliable values for electrons (Behrens *et al* 2009). In this work, calculations of the eye lens dose have been performed for photons incident on the head and trunk.

## 2. Materials and methods

### 2.1. Geometry and substances

The geometry and substances of the eye were taken from Behrens *et al* (2009). In that publication, the eye model of Charles and Brown (1975) was implemented which was adopted by ICRP (ICRP 2003). The dimensions of the eye are taken to be the mean values of those of the male and female eye (Charles and Brown 1975). Thus, the eye model of Behrens *et al* (2009) is used to calculate a single set of conversion coefficients representative of both sexes. In this geometry the radiation sensitive volume is located in the front region of the eye lens (mass: 39.2 mg; volume: 37.0 mm<sup>3</sup>; mean depth below the surface of the eye: 3.25 mm which is 3.36 mm tissue equivalent). The geometry of the head and body was adopted from Kramer *et al* (1982). To represent both sexes here, too, the dimensions were taken as mean values of the dimensions of the ADAM and EVA phantoms (Kramer *et al* 1982). The head and body serve to take into account absorption and scattered radiation. Therefore, the medium of the head and body was simply chosen to be ICRU 4-element standard tissue, however, with a density of 1.11 g cm<sup>-3</sup>. This mean density was deduced for the head from data from Bouchet *et al* (1999) and ICRP 103 (ICRP 2003). The omission of further details, e.g. bones especially in the vicinity of the eyes, is justified as no systematic deviations from calculations performed with anthropomorphic phantoms (REX and REGINA) were observed, see below. Details of the geometry definition of the head and body and of the position of the eyes in the head are given in appendix A. In figure 1, the geometry is shown as three-dimensional graphs.

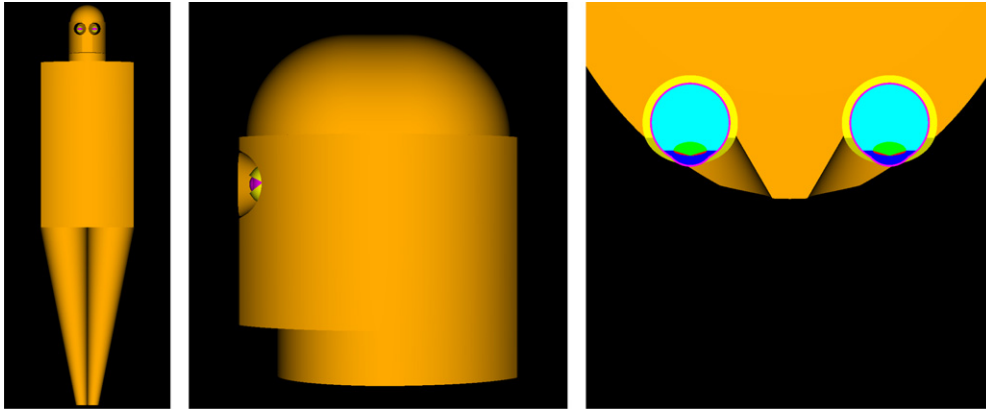


**Figure 1.** Views of the geometry used in the Monte Carlo simulations. Different colours indicate different materials. Left: complete body. Middle: head and eyes from the side. Right: head and eyes from the top with a cut at the centre of the eyes. The graphs were produced using egsp (Kawrakow 2005).

## 2.2. Method of calculation

The mean absorbed dose per photon fluence in the eye lens is determined using the transport code package EGSnrc, version V4-r2-3-0 (Kawrakow and Rogers 2006). The dose per fluence was calculated for different parts of the eye lens: the sensitive volume, the insensitive volume, and the entire lens. For the definition of the different volumes, see Behrens *et al* (2009). The geometry was implemented using egsp, the C++ class library of EGSnrc (Kawrakow 2005). The egsp code package was modified and used according to Behrens (2010). The cross section data for the electron transport (where the condensed history technique is applied) are Standard EGSnrc (based on the Bethe–Bloch theory) for the collision stopping power and Bethe–Heitler cross sections for the radiative stopping power. For photons, the standard EGSnrc cross sections are used (PEGS4, see the manual of EGSnrc (Kawrakow and Rogers 2006)). The most important particle transport parameters are the following. The maximum energy loss per electron step is 25% (ESTEPE = 0.25). Photons are followed down to an energy of 1 keV (PCUT = 0.001 MeV) and 10 keV (PCUT = 0.010 MeV) for initial photon energies below and above 510 keV, respectively. Electrons are followed down to a kinetic energy of 1 keV (ECUT = 0.512 MeV)<sup>3</sup> and 10 keV (ECUT = 0.521 MeV)<sup>3</sup>, for initial photon energies below and above 110 keV, respectively.

All calculations were performed for incident mono-energetic photons with the phantom in vacuum and a parallel radiation beam large enough to irradiate the head and trunk (the radiation scattered from the legs was also taken into account). A radiation incidence of 0° means that the beam is incident from the front onto the body and the eye looks into the beam. In table 1, the angles of incidence for which calculations were performed are listed.

For the calculations, a slightly modified version of ‘tutor2pp.cpp’ (a user code distributed with EGSnrc) was used. This code calculates the deposited energy per source particle,  $E_{\text{dep}}/N$ , in the different regions of the geometry. Equation (1) was used to obtain the equivalent dose per incident fluence,  $H_T/\Phi$ :

$$\frac{H_T}{\Phi} = \frac{E_{\text{dep}}}{N} \cdot \frac{A}{m} \cdot w_R \quad (1)$$

<sup>3</sup> ECUT includes the rest mass of the electron (511 keV) which has to be subtracted to obtain the kinetic energy.

**Table 1.** Angles of incidence (in the  $x$ - $y$  plane) for which calculations were performed.

Description	Nomenclature according to ICRP 74 (ICRP 1996)
Radiation incidence of $0^\circ$ (see the left part of figure 1)	AP
Radiation incidence of $45^\circ$	–
Radiation incidence of $90^\circ$ (mean value of incidence from the left and the right)	LAT
Radiation incidence from the left (see the middle part of figure 1)	LLAT
Radiation incidence of $180^\circ$	PA
Radiation incidence from $0^\circ$ to $355^\circ$ in steps of $5^\circ$ <sup>a</sup>	ROT

<sup>a</sup> The results of these calculations were averaged representing an irradiation with a stationary parallel beam while the phantom is rotated about the long axis of the body. To confirm this procedure, the values for  $0^\circ$  to  $350^\circ$  in steps of  $10^\circ$  were averaged, too, leading to the same results.

where  $A$  is the cross-sectional area of the incident radiation beam,  $m$  is the mass of the corresponding region (calculated separately), and  $w_R$  is the radiation weighting factor for photons ( $w_R = 1$ ). To obtain the conversion coefficients from air kerma to dose from the calculated values, the following equation was used:

$$\frac{H_T}{K_a} = \frac{H_T/\Phi}{K_a/\Phi} = \frac{H_T/\Phi}{(\mu_{en}/\rho) \cdot E} \quad (2)$$

where  $H_T/\Phi$  is the dose per incident fluence,  $\mu_{en}/\rho$  is the energy absorption coefficient taken from Hubbell and Seltzer (1995), and  $E$  is the photon energy. Values for  $(\mu_{en}/\rho) \cdot E$  are given in table B1 of appendix B.

Calculations were carried out at the same photon energies for which conversion coefficients in ICRP 74 are available. In addition, values for some further photon energies were calculated.

### 2.3. Uncertainty of calculations

As usual for Monte Carlo particle transport codes, EGSnrc only supplies statistical standard deviations. To assess other contributions to the overall uncertainty<sup>4</sup>, the most important transport parameters were varied, see table 2, and calculations were performed. The resulting mean conversion coefficients are consistent within their two sigma statistical uncertainties with the values obtained using the original parameters. Only at photon energies below 40 keV did the values obtained with the XCOM photon cross sections deviate by up to  $\pm 9\%$  from the values obtained with the EGSnrc standard photon cross sections. Therefore, an additional uncertainty contribution of 3% is assumed in this energy region.

The remaining non-statistical contributions are estimated to be about 2% due to general experiences in Monte Carlo transport calculations. Thus, the total non-statistical uncertainty is estimated to be 2% (3.6% below 40 keV).

To obtain the overall uncertainty of the calculated conversion coefficients, the squares of the contributions due to statistics and the non-statistical contribution have been added and the square root is calculated of the corresponding sum.

<sup>4</sup> The term ‘uncertainty’ is used in a general way: it contains the ‘standard deviation’ but contributions that are not determined by means of statistics are contained too.

**Table 2.** Monte Carlo parameters modified to assess the systematic uncertainties.

Parameter	Explanation	Original parameter	Modified parameter
ESTEPE	Maximum relative energy loss per electron step	0.25 (= 25%)	0.05 (= 5%)
PCUT and ECUT	Energy down to which photons are followed and energy down to which electrons are followed	1 keV for $E_{\text{ph}} < 510$ keV 10 keV for $E_{\text{ph}} > 510$ keV and 512 keV <sup>a</sup> for $E_{\text{el}} < 110$ keV 521 keV <sup>a</sup> for $E_{\text{el}} > 110$ keV	1 keV for all photon energies and 512 keV <sup>a</sup> for all photon energies
Data library for the photon cross sections		Standard EGSnrc	XCOM <sup>b</sup>

<sup>a</sup> ECUT includes the rest mass of the electron (511 keV) which has to be subtracted to obtain the kinetic energy.

<sup>b</sup> The XCOM cross sections are based on newer data from Berger and Hubbell (1987) from NIST.

### 3. Results

#### 3.1. Results for different angles of incidence (mean values of both eyes)

In figures 2–6 and tables B2–B6 (see appendix B), the equivalent dose per air kerma and the equivalent dose per photon fluence, respectively, are given for the sensitive volume of the lens, the insensitive volume of the lens, and the entire lens. Always, the mean value for the two eyes is given. The error bars according to the overall uncertainties are smaller than the symbols used; thus, they are not shown. The dose to the sensitive volume of the lens is most relevant in radiation protection. Therefore, these values are compared to the values for the ADAM phantom given in ICRP 74 (ICRP 1996) and to the values for the new reference computational male and female voxel phantoms (Rex and Regina) given by Schlattl *et al* (2007); see figures 2–5 (right parts). The following features can be seen.

- The values for the different parts of the lens (left parts of figures 2–6) are quite similar. Only for 0° angle of incidence, the values for the sensitive volume (front part of the lens) are slightly larger than those for the insensitive volume (rear part of the lens) for photon energies below 40 keV. The reason is photon absorption in the front part of the lens. In contrast, above the photon energy of about 1 MeV, the values for the front part are smaller than those for the rear part. The reason is the dose build-up effect which is stronger for larger photon energies. The values for the entire lens are always between the values for the front and rear part of the lens, as these two contributions are averaged.
- The values for the ADAM phantom are larger than the values of this work for photon energies below 40 keV by up to a factor of 1.6 at 10 keV and 0° angle of incidence and by up to a factor of 5 at 10 keV and 90° angle of incidence (see the right parts of figures 2, 3 and 5). The reason is that the lenses of the ADAM phantom are not covered by tissue because they are modelled by a small tissue, volume at the surface of the head. For PA incidence (see figure 4) the values are nearly equal as only radiation coming through the back of the head contributes to this.
- For AP incidence and photon energies above about 1 MeV, the values for the ADAM phantom are larger than the values of this work by up to a factor of 7 at 10 MeV. The

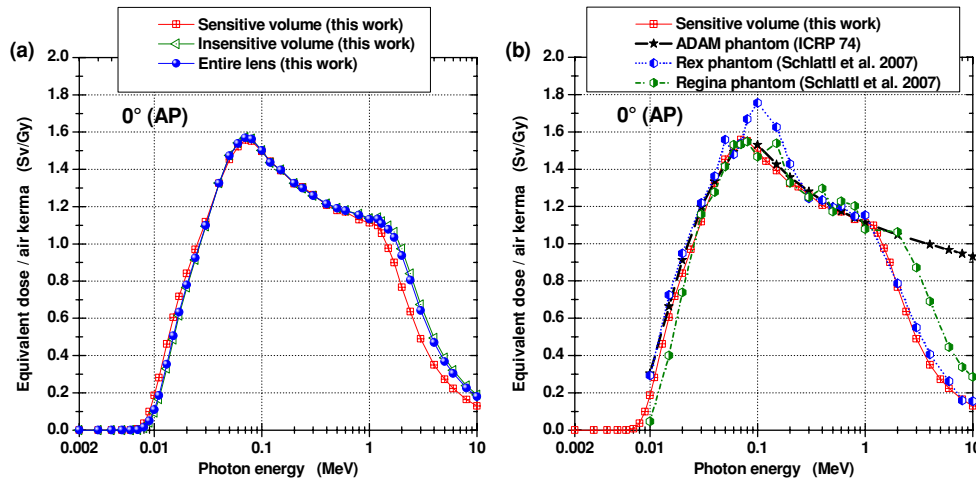


**Figure 2.** Equivalent dose per air kerma for  $0^\circ$  angle of incidence (AP) for different parts of the lens: (a) this work and (b) in comparison to other data.

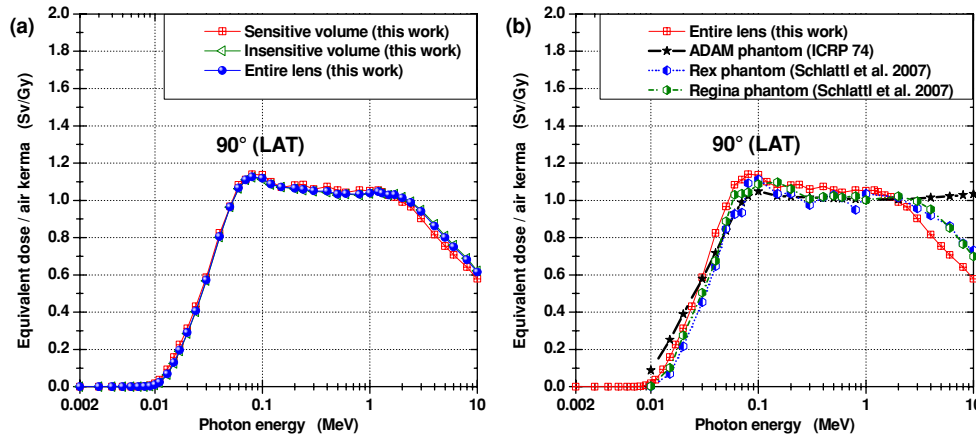


**Figure 3.** Equivalent dose per air kerma for  $90^\circ$  angle of radiation incidence (LAT) for different parts of the lens: (a) this work and (b) in comparison to other data.

reason is that the calculations with the ADAM phantom were performed using kerma approximation (KA), which means that no secondary electrons are transported, but their energy is deposited in the calculation at the place of their creation. Therefore, the dose is—at any position within the ADAM phantom—always as large as if the build-up effect was completed. In this work, the secondary electrons are properly followed and thus the dose build-up is not finished in the eye lens for high energy photons, resulting in smaller values. This topic is discussed in further detail in section 4.

- The values for the Rex and Regina phantoms are roughly equivalent to the values of this work as these values were calculated including the transport of the secondary electrons. However, it is obvious that especially for AP incidence and for photon energies below about 60 keV, the values of the Rex phantom are larger than those of the Regina phantom, while for photon energies above about 1 MeV the opposite is true. The reason is that the voxel size is different in the two phantoms resulting in different photon absorptions and dose build-up at photon energies below 60 keV and above 1 MeV, respectively.

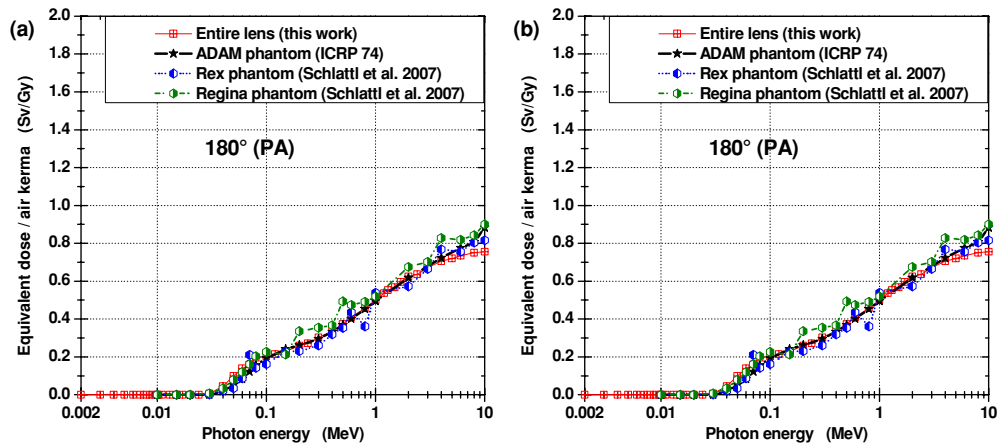


**Figure 4.** Equivalent dose per air kerma for  $180^\circ$  angle of radiation incidence (PA) for different parts of the lens: (a) this work and (b) in comparison to other data.

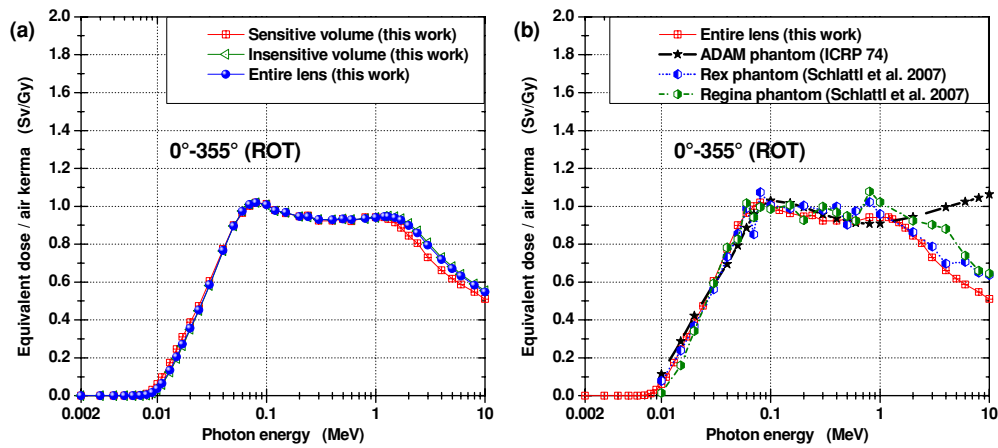


**Figure 5.** Mean equivalent dose per air kerma for radiation incidence from  $0^\circ$  to  $355^\circ$  in steps of  $5^\circ$  (ROT) for different parts of the lens: (a) this work and (b) in comparison to other data.

In summary, it can be said that the values calculated for the different phantoms roughly agree except for photon energies above 1 MeV where the values for the ADAM phantom significantly deviate due to the method of calculation.

In figure 7, values calculated in this work for the sensitive part of the lens are shown for different directions of radiation incidence. It can be seen that with rising angles of incidence the values grow smaller for photon energies below a few MeV due to photon absorption, and that they grow larger for photon energies above a few MeV due to the dose build-up effect.

### 3.2. Results for the left and right eye

For  $45^\circ$  and  $90^\circ$  angles of radiation incidence, the geometry is not symmetric with respect to the two eyes. Therefore, in figure 8 the values for these two angles of incidence are presented for the two eyes. It can be seen that especially for the  $90^\circ$  angle of incidence (LLAT), the different



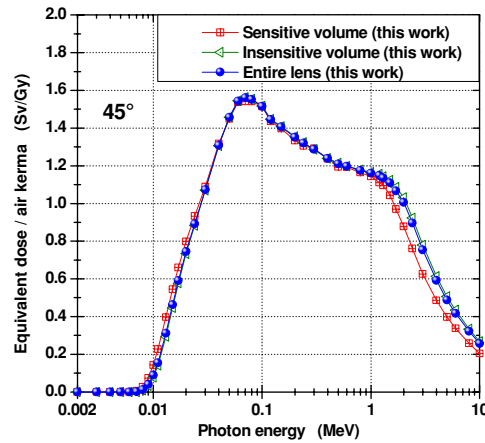


**Figure 6.** Equivalent dose per air kerma for  $45^\circ$  angle of radiation incidence for different parts of the lens (this work).

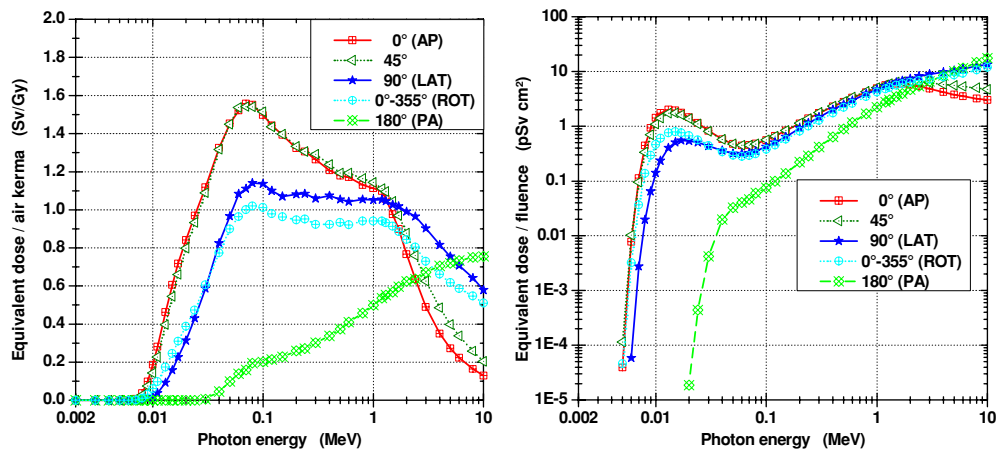


**Figure 7.** Equivalent dose per air kerma (left) and equivalent dose per incident fluence (right) for different directions of radiation incidence for the sensitive part of the lens. The mean values for the two eyes are given.

amount of material in front of the left and right eye results in different photon absorption and dose build-up for photon energies below and above a few MeV, respectively. This can be seen even better in figure 9 where the angular dependence is given for four photon energies for the sensitive volume of the left eye. For 0.02 and 0.1 MeV, photon energy absorption dominates resulting in large dose values for irradiations from the front, while, however, at 10 MeV photon energy the dose build-up dominates resulting in large dose values for irradiations from the back and from the right (opposite the eye under consideration). The corresponding graph for the right eye is identical to figure 9 except for the lines that are mirrored at the horizontal axis connecting  $180^\circ$  and  $0^\circ$ .

In the case of a high dose exposure, cataract induction due to deterministic effects is important. If a high dose exposure occurs mainly from one side of the body, it might be necessary to distinguish between the doses to the two eyes. Therefore, in table B7 of appendix B, values for both eyes are given for the LLAT geometry. For  $60^\circ$  and smaller

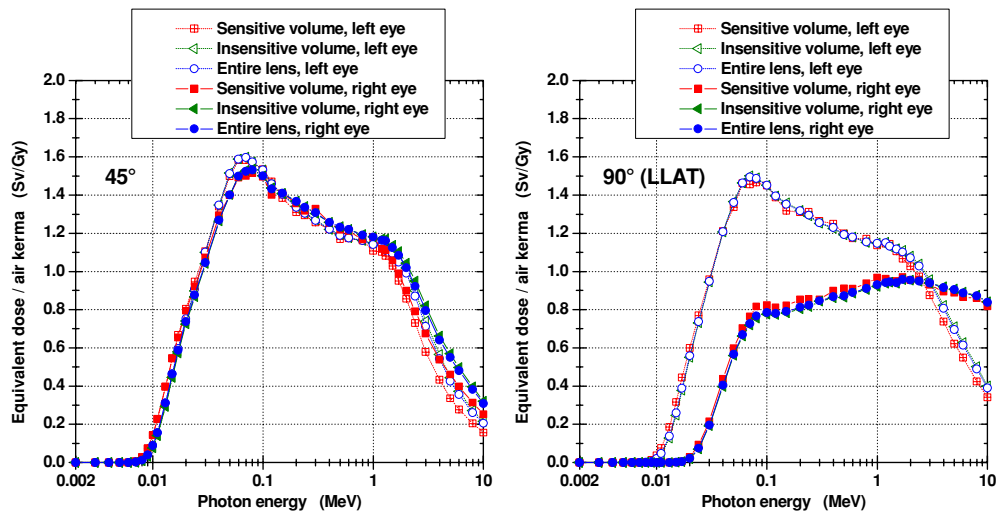


**Figure 8.** Equivalent dose per air kerma for 45° and 90° angles of incidence for different parts of the lens and for the two eyes. Radiation incidence is from the left (LLAT).

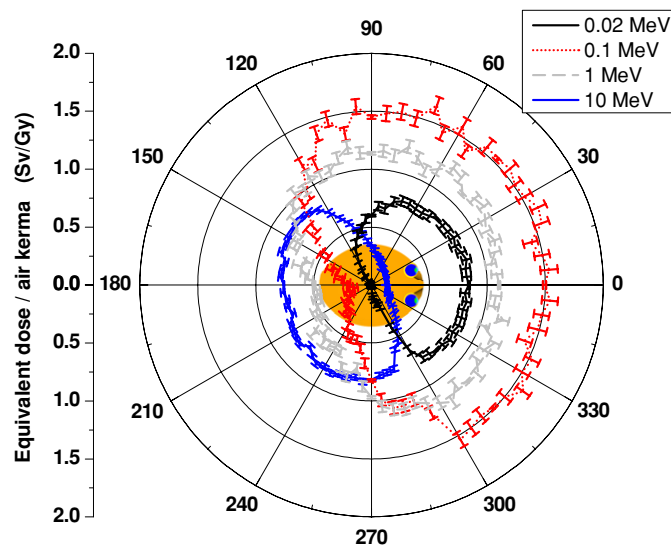


**Figure 9.** Angular dependence of the equivalent dose per air kerma for different photon energies for the sensitive part of the lens of the left eye. To illustrate the irradiation geometry, the head cut at the centre of the eyes is shown from the top. The error bars give the one sigma standard deviation due to statistical fluctuations (see section 2.3) which are relatively large due to limited computing time.

angles of incidence, the difference of the two eyes is negligible; see figures 8 and 9 (where in figure 9 the conversion coefficients at angles  $\theta$  and  $360^\circ - \theta$  are similar, which means that the dose values for the two eyes are similar).

### 3.3. Contributions from the head and the trunk

In order to assess the contributions from the different parts of the body to the eye lens dose, calculations were performed separately for the irradiation of the head and the trunk. It turned out that the contribution of the trunk to the total dose was less than 1% for angles of radiation incidence below about 135°, about 3% at 160° and about 4% at 180°. The maximal contribution was observed for about 100 keV photon energy corresponding to the well-known fact that in this energy region, the Compton cross section has its maximum. Due to this very small contribution of the trunk, no separate calculations were performed for the irradiation of the legs which, however, were always included in the simulation geometry (see section 2.2).

## 4. Usage of the conversion coefficients (Kerma approximation (KA): pros and cons)

As stated above, secondary electrons were taken into account which means that no KA was used. This is usual for nowadays calculations of conversion coefficients for photons in order to assess doses correctly at interfaces of different materials within the body (Schlatzl *et al* 2007)<sup>5</sup>. In addition, the calculations were performed with the phantom in vacuum. That means the conversion coefficients are valid for pure photon radiation fields without any secondary electrons at the surface of a person. In a real radiation field, however, secondary electrons may be present due to the material located between the photon source and the person. In particular, for persons wearing glasses, the amounts of secondary electrons produced outside the body are not negligible. This fact is important for photon energies above about 1 MeV (depending on the angle of radiation incidence) where the dose build-up in the eye is not finished in front of the eye lens. This can be seen in figure 10, where, for the AP and LAT geometry, the conversion coefficients from photon fluence to eye lens dose for the sensitive volume of the eye lens are shown for calculations with and without KA. For the former calculation the transport parameter ECUT was set to 10.511 MeV, resulting in no secondary electron transport at all, while their energy is deposited at the place of their creation. In addition, the data from ICRP 74 (ICRP 1996) are shown. It can be seen that the values of this work calculated with KA are similar to the values from ICRP 74 up to about 1 MeV photon energy. Above this energy, they are larger by up to 20% for the AP geometry. However, this difference is negligible compared to the difference to the values calculated without KA (about a factor of 5).

As a consequence, three methods to assess dose values from fluence spectra in photon radiation fields are possible.

- (1) *Accurate method.* Both contributions to the radiation field, the fluence of photons and electrons incident on the surface of the body at the point of interest, have to be assessed. Then the eye lens dose due to photons has to be calculated using the conversion coefficients presented in this work. In addition, the eye lens dose due to electrons has to be calculated using the conversion coefficients presented earlier, Behrens *et al* (2009) and corrigendum. These two dose contributions have to be added up to obtain the total eye lens dose.
- (2) *Approximate method* if it is assumed that none or only a few secondary electrons are produced between the photon source and the body. The fluence of photons incident on the surface of the body at the point of interest has to be assessed. Then the eye lens dose has to be calculated using the conversion coefficients presented in this work.
- (3) *Approximate method* if it is assumed that a considerable contribution of secondary electrons is produced between the photon source and the body. The fluence of photons

<sup>5</sup> This is different for the values presented in ICRP 74 (ICRP 1996), where the kerma approximation was used in order to save computing time.

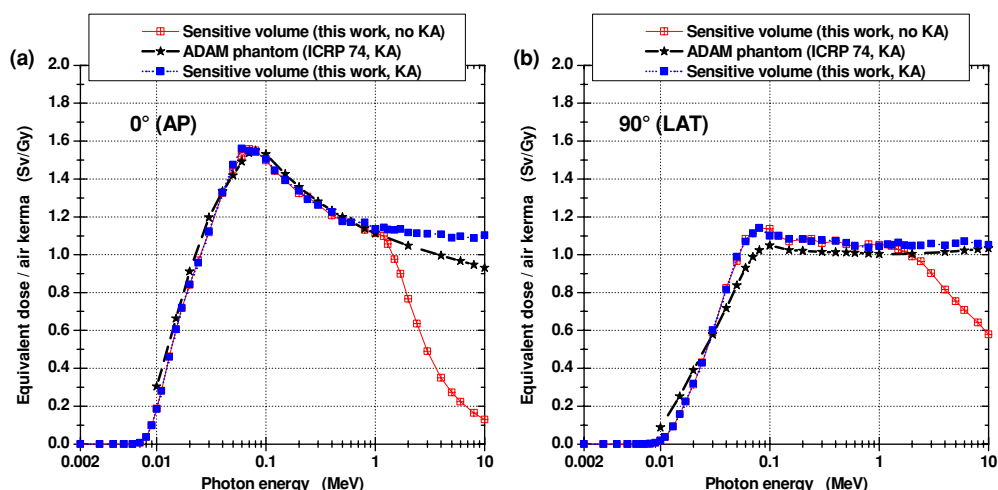


**Figure 10.** Equivalent dose per air kerma for the AP and LAT geometries calculated with and without KA.

incident on the surface of the body at the point of interest has to be assessed. Then, for photons with energies below 1 MeV, the eye lens dose has to be calculated using the conversion coefficients presented in this work. For photons with energies above 1 MeV, the conversion coefficients given in ICRP 74 (ICRP 1996) may be used, as these values are nearly equal to the values calculated in this work using KA (see figure 10). Therefore, no tables of conversion coefficients calculated with KA are given in this work. This method is a conservative estimation of the dose. It shall only be applied in case the amount of secondary electrons cannot be estimated. In case that is possible, method 1 should be preferred as more accurate dose values result.

Depending on the amount and on the type of material in front of the person, for photons above 1 MeV the real eye lens dose (calculated according to the first method) may even be larger than the dose calculated according to the third method. The reason is that the yield of secondary electrons emitted by material with a high atomic number (for example, contained in glasses with large refraction indices and in protective lead glasses) may be higher than the yield produced by tissue material of the eye. The latter tissue, however, is used in the calculation with KA.

## 5. Discussion and conclusions

For the first time, calculations of the dose to the sensitive volume in the lens were performed for photon radiation using a realistic eye model and taking into account the well-known fact that the sensitivity of the eye lens with respect to cataract induction is highly inhomogeneous within the lens. From these calculations, conversion coefficients from fluence (and air kerma) to equivalent dose of the eye lens were deduced. Below 40 keV and above 1 MeV, photon energy significant differences occur between the values of the sensitive and insensitive volume of the lens: for example, at 10 keV and 0° angle of incidence, they differ by a factor of 2.

Between photon energies 40 keV and 1 MeV, the calculated values are in good agreement with those calculated by Schlattl *et al* (2007) using the new ICRP voxel phantoms and with those published in ICRP 74 (ICRP 1996). However, at photon energies below 40 keV and above

1 MeV, they are up to a factor of 5 smaller (at 10 keV at the LAT geometry and at 10 MeV at the AP geometry) than the values published in ICRP 74 (ICRP 1996), where the KA was used.

In section 4, the pros and cons of using or not using the KA were discussed leading to detailed recommendations on how to obtain a realistic eye lens dose from fluence spectra taking into account the contribution from secondary electrons.

The question of which dose quantity should be used to monitor the exposure of the eye lens was discussed by Behrens and Dietze (2010). There the values presented in ICRP 74 for the AP geometry ( $0^\circ$  angle of incidence) were taken as basic values to which different operational quantities were compared for realistic photon radiation fields with photon energies up to about 1 MeV. As in this energy region, the new values for the conversion coefficients are quite similar to those in ICRP 74, the conclusions drawn by Behrens and Dietze (2010) are still valid: in photon radiation fields, especially x-ray fields, both quantities  $H_p(0.07)$  and  $H_p(3)$  are suitable to monitor the exposure of the eye lens if the dosimeters are calibrated on a slab phantom for simulating the backscattering situation of the head.

## Acknowledgments

The authors wish to thank the Task Group 4 on Dose Calculations (DOCAL) of the International Commission on Radiological Protection (ICRP) for inspiring this work. In addition, the authors are grateful to Peter Ambrosi (PTB) for very helpful discussions.

## Appendix A. Mathematical definition of the geometry used for the particle transport simulation

### A.1. General

The mathematical model of the ADAM phantom presented by Kramer *et al* (1982) was used. The phantom is positioned in the mathematical coordinated systems as follows: the origin of the coordinate system is located at the bottom of the trunk at the centre where the legs touch each other. The long axis of the phantom lies parallel to the  $z$ -axis (the head in the positive  $z$ -direction), the front face of the phantom looks into the negative  $y$ -direction, the left side of the phantom is directed to the positive  $x$ -direction. To represent both sexes, the dimensions were taken as the mean values of the dimensions of the ADAM and EVA phantoms, in the following called the ADAM-EVA phantom. The ADAM-EVA phantom utilizes several elliptical shapes; however, in EGSpp no elliptical geometries are possible. Therefore, these parts of the geometry were approximated by intersecting cylinders and spheres (see below).

### A.2. Head

Citation from Kramer *et al* (1982): ‘The head consists of a right elliptical cylinder topped by half an ellipsoid. At the lower section of the cylinder a part is removed to represent the chin.

- Upper part of head:  $84.5 \text{ cm} < z : \left(\frac{x}{7.75 \text{ cm}}\right)^2 + \left(\frac{y}{9.7 \text{ cm}}\right)^2 + \left(\frac{z-84.5 \text{ cm}}{7 \text{ cm}}\right)^2 \leq 1$ .
- Middle part of head:  $71.6 \text{ cm} < z \leq 84.5 \text{ cm} : \left(\frac{x}{7.75 \text{ cm}}\right)^2 + \left(\frac{y}{9.7 \text{ cm}}\right)^2 \leq 1$ .
- Lower part of head:  $68 \text{ cm} \leq z \leq 71.6 \text{ cm} :$ 
  - Rear part:  $y \geq 0 : \left(\frac{x}{7.75 \text{ cm}}\right)^2 + \left(\frac{y}{9.7 \text{ cm}}\right)^2 \leq 1$
  - Front part:  $y < 0 : \left(\frac{x}{7.75 \text{ cm}}\right)^2 + \left(\frac{y}{6.8 \text{ cm}}\right)^2 \leq 1$ .

The implementation in EGSpp consists of the following geometries.

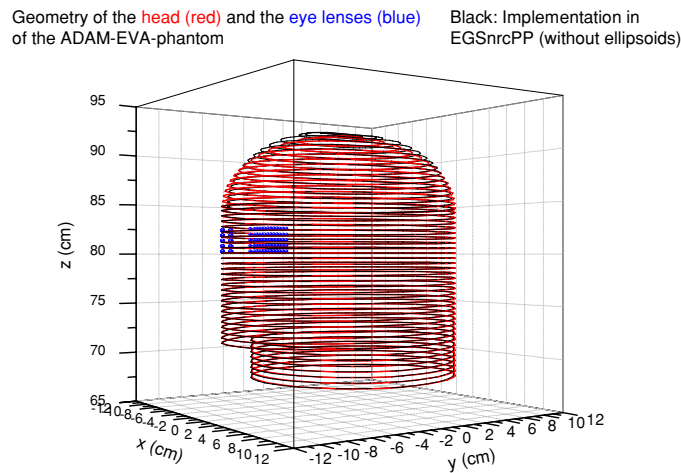


**Figure A1.** Illustration of the geometry of the head according to the ADAM-EVA phantom (red) and its implementation in EGSpp (black: slightly deviating as in EGSpp no elliptical geometries are possible). The eye lenses are shown for information only.

- Upper part of the head: two quarter spheres connected with a half cylinder,  $z > 84.5$  cm.  
Midpoints of the two spheres:  $(x ; y ; z) = (0 \text{ cm} ; \pm 1.95 \text{ cm} ; 84.5 \text{ cm})$   
Radii of the two spheres:  $r = 7.2$  cm. Valid values for  $y$ :  $|y| > 1.95$  cm  
Cylinder along the  $y$ -axis:  $r = 7.2$  cm. Valid values for  $y$ :  $|y| \leq 1.95$  cm.
- Middle part of the head: three intersecting cylinders along the  $z$ -axis. Only the region that is covered by all three cylinders is taken as the volume,  $71.6 \text{ cm} < z \leq 84.5$  cm.  
Two cylinders: midpoints and radii:  $(x ; y) = (\pm 3.036 \text{ cm} ; 0 \text{ cm})$  and  $r = 10.79$  cm  
Third cylinder: midpoint and radius:  $(x ; y) = (0 \text{ cm} ; 0 \text{ cm})$  and  $r = 9.7$  cm
- Lower part of the head (cervix):  $68 \text{ cm} \leq z \leq 71.6$  cm.  
Rear part: the rear part (neck) is constructed in the same way as the middle part of the head; however, only values for  $y > 0$  cm are valid.  
Front part: the front part consists of one cylinder:  
midpoint and radius:  $(x ; y) = (0 \text{ cm} ; -0.79 \text{ cm})$  and  $r = 7.79$  cm; only values for  $y \leq 0$  cm are valid.

Figure A1 illustrates that the implementation in EGSpp approximates the geometry quite well. The eye lenses of the ADAM-EVA phantom are just shown for information. As stated in section 3.1, they consist of a small piece of tissue at the surface of the head; no further details of the eyes are implemented in the ADAM-EVA phantom.

### A.3. Positions of the eyes in the head and implementation of eye sockets

The centres of the eyeballs (denoted as  $M = 0$  in figure 1 in the paper of Behrens *et al* (2009)) are located at the following positions in the head:  $(x ; y ; z) = (\pm 3 \text{ cm} ; -7.4 \text{ cm} ; 81.25 \text{ cm})$ . The ‘ $\pm$ ’ sign is taken as plus for the left eye and minus for the right eye, respectively.

In order to represent the eye sockets, a section of the head in the form of a cone made of vacuum is cut out in front of each eye, see figure 1. The cones are defined as follows: apexes:  $(x ; y ; z) = (\pm 3 \text{ cm} ; -5.4 \text{ cm} ; 81.25 \text{ cm})$ . The axes lie parallel to the  $y$ -axis. Opening angle:  $30^\circ$ . Only values for  $y < -7.4$  cm are taken.

#### A.4. Trunk

Citation from Kramer *et al* (1982): ‘The trunk is represented by an elliptical cylinder specified by  $(\frac{x}{19.4 \text{ cm}})^2 + (\frac{y}{9.7 \text{ cm}})^2 \leq 1$  and  $0 < z \leq 68 \text{ cm}$ ’.  
The implementation in EGSpp is as follows.

- Three intersecting cylinders along the  $z$ -axis. Only the region that is covered by all three cylinders is taken as the volume,  $0 \text{ cm} < z \leq 68 \text{ cm}$  :  
Two cylinders: midpoints and radii:  $(x ; y) = (0 \text{ cm} ; \pm 21.25 \text{ cm})$  and  $r = 30.95 \text{ cm}$   
Third cylinder: midpoint and radius:  $(x ; y) = (0 \text{ cm} ; 0 \text{ cm})$  and  $r = 19.4 \text{ cm}$ .

#### A.5. Legs

Citation from Kramer *et al* (1982): ‘The legs are represented by the frustums of two circular cones:  $x^2 + y^2 \leq \pm x \cdot (19.4 \text{ cm} + 2 \cdot z)$  and  $-73.5 \text{ cm} \leq z \leq 0$ . The ‘ $\pm$ ’ sign is taken as plus for the left leg and minus for the right leg, respectively’. The implementation in EGSpp is the same.

### Appendix B. Tables with the kerma coefficients and the calculated values of the mean absorbed dose per incident electron fluence

The tables provide kerma coefficients and conversion coefficients for a set of specific energies. Interpolation between values at given energies should be performed using a log–log interpolation.

**Table B1.** Kerma coefficients,  $K_a/\Phi = (\mu_{\text{en}}/\rho) \cdot E$ , used for the conversion from dose per fluence to dose per air kerma (section 2.2, equation (2)). The values for  $(\mu_{\text{en}}/\rho)$  are taken from Hubbell and Seltzer (1995). The numerical equation  $\frac{K_a}{\Phi} = \frac{\mu_{\text{en}}}{\rho} \cdot E \cdot 160.21$  with  $\frac{K_a}{\Phi}$  in pGy cm<sup>2</sup>,  $\frac{\mu_{\text{en}}}{\rho}$  in cm<sup>2</sup> g<sup>-1</sup>, and  $E$  in MeV was used. The number 160.21 follows from the conversion of MeV cm<sup>2</sup> g<sup>-1</sup> to pGy cm<sup>2</sup>. The values written in bold italics are obtained by interpolation as no values for  $(\mu_{\text{en}}/\rho)$  are available<sup>a</sup>.

Photon energy $E$ (MeV)	Kerma coefficient (pGy cm <sup>2</sup> )	Photon energy $E$ (MeV)	Kerma coefficient (pGy cm <sup>2</sup> )
0.005	31.49	0.200	0.8562
0.006	21.82	<b><i>0.240</i></b>	<b><i>1.061</i></b>
<b><i>0.007</i></b>	<b><i>15.92</i></b>	0.300	1.380
0.008	12.11	0.400	1.890
<b><i>0.009</i></b>	<b><i>9.468</i></b>	0.500	2.376
0.010	7.597	0.600	2.839
<b><i>0.011</i></b>	<b><i>6.203</i></b>	0.800	3.694
<b><i>0.013</i></b>	<b><i>4.347</i></b>	1.000	4.468
0.015	3.206	<b><i>1.200</i></b>	<b><i>5.147</i></b>
<b><i>0.017</i></b>	<b><i>2.449</i></b>	<b><i>1.300</i></b>	<b><i>5.477</i></b>
0.020	1.727	1.500	6.120
<b><i>0.024</i></b>	<b><i>1.179</i></b>	<b><i>1.700</i></b>	<b><i>6.692</i></b>
0.030	0.7387	2.000	7.514
0.040	0.4379	<b><i>2.400</i></b>	<b><i>8.501</i></b>

**Table B1.** (Continued.)

Photon energy $E$ (MeV)	Kerma coefficient (pGy cm <sup>2</sup> )	Photon energy $E$ (MeV)	Kerma coefficient (pGy cm <sup>2</sup> )
0.050	0.3283	3.000	9.887
0.060	0.2923	4.000	11.98
<b>0.070</b>	<b>0.2902</b>	5.000	13.94
0.080	0.3085	6.000	15.83
0.100	0.3725	8.000	19.55
<b>0.120</b>	<b>0.4615</b>	10.000	23.23
0.150	0.5998		

<sup>a</sup> A log–log interpolation was used except for 70 keV. At this energy, the values take a minimum resulting in a curved energy dependence. Therefore, a natural cubic spline was used for this energy.

**Table B2.** Equivalent dose per photon fluence for the sensitive volume of the lens,  $H_s/\Phi$ , for the insensitive volume of the lens,  $H_i/\Phi$ , and for the entire lens of the eye,  $H_e/\Phi$ , for mono-energetic photons and AP exposure (0°) of the head and trunk. The values in brackets are the statistical one sigma standard uncertainties (absolute values of the most right digit, e.g. ‘0.00775 (20)’ means ‘0.00775 ± 0.00020’). The overall uncertainty is the geometrical sum of the statistical uncertainty and the non-statistical uncertainty which is estimated to be 2% (3.6% below 40 keV), see section 2.3.

Photon energy (MeV)	Equivalent dose per photon fluence (pSv cm <sup>2</sup> ) to the		
	sensitive volume $H_s/\Phi$	insensitive volume $H_i/\Phi$	entire lens $H_e/\Phi$
0.005	0.000 039 (13)	0 (–)	0.000 007 (3)
0.006	0.007 75 (20)	0.000 81 (3)	0.002 00 (5)
0.007	0.1127 (8)	0.021 82 (16)	0.037 38 (19)
0.008	0.4460 (17)	0.1307 (5)	0.1846 (5)
0.009	0.937 (3)	0.3794 (8)	0.4749 (8)
0.010	1.416 (4)	0.7126 (11)	0.8330 (11)
0.011	1.749 (4)	1.0316 (14)	1.1545 (14)
0.013	2.009 (5)	1.4389 (18)	1.5365 (17)
0.015	1.940 (5)	1.5600 (20)	1.6250 (19)
0.017	1.758 (5)	1.507 (3)	1.5502 (19)
0.020	1.453 (5)	1.323 (3)	1.3451 (19)
0.024	1.143 (6)	1.077 (3)	1.089 (3)
0.030	0.826 (5)	0.8086 (19)	0.8116 (18)
0.040	0.580 (4)	0.5806 (18)	0.5805 (16)
0.050	0.477 (4)	0.4845 (17)	0.4832 (15)
0.060	0.445 (4)	0.4507 (16)	0.4497 (15)
0.070	0.452 (4)	0.4560 (16)	0.4554 (14)
0.080	0.478 (4)	0.4826 (16)	0.4818 (15)
0.100	0.557 (4)	0.5595 (17)	0.5592 (15)
0.120	0.666 (5)	0.662 (3)	0.6629 (20)
0.150	0.835 (5)	0.838 (3)	0.838 (3)
0.200	1.133 (8)	1.135 (4)	1.134 (3)



**Table B2.** (Continued.)

Photon energy (MeV)	Equivalent dose per photon fluence (pSv cm <sup>2</sup> ) to the		
	sensitive volume $H_s/\Phi$	insensitive volume $H_i/\Phi$	entire lens $H_e/\Phi$
0.240	1.386 (10)	1.377 (5)	1.379 (5)
0.300	1.744 (12)	1.736 (6)	1.737 (5)
0.400	2.281 (16)	2.297 (8)	2.295 (7)
0.500	2.801 (20)	2.833 (10)	2.828 (9)
0.600	3.33 (3)	3.347 (12)	3.343 (11)
0.800	4.18 (3)	4.283 (16)	4.264 (14)
1.000	4.97 (4)	5.075 (20)	5.057 (17)
1.200	5.66 (4)	5.87 (3)	5.835 (20)
1.300	5.79 (4)	6.13 (3)	6.07 (3)
1.500	5.97 (4)	6.72 (3)	6.59 (3)
1.700	6.02 (4)	7.11 (3)	6.92 (3)
2.000	5.76 (4)	7.31 (3)	7.04 (3)
2.400	5.41 (4)	7.14 (4)	6.84 (3)
3.000	4.84 (3)	6.66 (3)	6.35 (3)
4.000	4.20 (3)	5.92 (3)	5.62 (3)
5.000	3.80 (3)	5.40 (3)	5.13 (3)
6.000	3.53 (3)	5.09 (3)	4.82 (3)
8.000	3.22 (3)	4.67 (3)	4.42 (2)
10.000	3.02 (3)	4.41 (3)	4.17 (2)

**Table B3.** Equivalent dose per photon fluence for the sensitive volume of the lens,  $H_s/\Phi$ , for the insensitive volume of the lens,  $H_i/\Phi$ , and for the entire lens of the eye,  $H_e/\Phi$ , for mono-energetic photons and LAT exposure (90°) of the head and trunk. The values in brackets are the statistical one sigma standard uncertainties (absolute values of the most right digit, e.g. '0.00775 (20)' means '0.00775 ± 0.00020'). The overall uncertainty is the geometrical sum of the statistical uncertainty and the non-statistical uncertainty which is estimated to be 2% (3.6% below 40 keV), see section 2.3.

Photon energy (MeV)	Equivalent dose per photon fluence (pSv cm <sup>2</sup> ) to the		
	sensitive volume $H_s/\Phi$	insensitive volume $H_i/\Phi$	entire lens $H_e/\Phi$
0.005	0 (-)	0 (-)	0 (-)
0.006	0.000059 (19)	0.0000024 (18)	0.000012 (4)
0.007	0.00275 (14)	0.00049 (3)	0.00088 (4)
0.008	0.0197 (4)	0.00477 (9)	0.00734 (10)
0.009	0.0648 (8)	0.0222 (3)	0.0295 (3)
0.010	0.1412 (12)	0.0627 (4)	0.0762 (4)
0.011	0.2339 (16)	0.1260 (6)	0.1445 (6)
0.013	0.405 (3)	0.2775 (9)	0.2993 (9)

**Table B3.** (Continued.)

Photon energy (MeV)	Equivalent dose per photon fluence (pSv cm <sup>2</sup> ) to the		
	sensitive volume $H_s/\Phi$	insensitive volume $H_i/\Phi$	entire lens $H_e/\Phi$
0.015	0.509 (3)	0.3978 (11)	0.4168 (11)
0.017	0.552 (4)	0.4667 (13)	0.4813 (12)
0.020	0.542 (4)	0.4920 (14)	0.5005 (13)
0.024	0.508 (4)	0.4724 (15)	0.4785 (14)
0.030	0.434 (4)	0.4197 (16)	0.4221 (14)
0.040	0.361 (4)	0.3512 (16)	0.3529 (14)
0.050	0.318 (4)	0.3163 (15)	0.3165 (14)
0.060	0.317 (4)	0.3106 (15)	0.3116 (14)
0.070	0.322 (4)	0.3221 (15)	0.3221 (14)
0.080	0.352 (4)	0.3465 (15)	0.3474 (14)
0.100	0.423 (4)	0.4150 (16)	0.4164 (15)
0.120	0.507 (4)	0.5006 (18)	0.5017 (17)
0.150	0.642 (5)	0.642 (3)	0.642 (3)
0.200	0.926 (8)	0.909 (4)	0.912 (3)
0.240	1.150 (10)	1.118 (5)	1.123 (4)
0.300	1.462 (12)	1.447 (6)	1.449 (5)
0.400	2.031 (17)	1.972 (8)	1.982 (8)
0.500	2.51 (3)	2.443 (11)	2.454 (10)
0.600	2.96 (3)	2.934 (13)	2.938 (12)
0.800	3.89 (4)	3.797 (17)	3.814 (15)
1.000	4.70 (4)	4.62 (3)	4.637 (19)
1.200	5.42 (5)	5.38 (3)	5.39 (3)
1.300	5.72 (5)	5.68 (3)	5.68 (3)
1.500	6.28 (5)	6.29 (3)	6.29 (3)
1.700	6.81 (5)	6.91 (4)	6.90 (3)
2.000	7.44 (6)	7.65 (4)	7.61 (4)
2.400	8.21 (6)	8.44 (4)	8.40 (4)
3.000	8.92 (6)	9.38 (5)	9.30 (4)
4.000	9.77 (7)	10.44 (5)	10.33 (4)
5.000	10.52 (7)	11.29 (5)	11.16 (5)
6.000	11.20 (7)	12.02 (6)	11.88 (5)
8.000	12.55 (8)	13.47 (6)	13.31 (5)
10.000	13.46 (8)	14.44 (6)	14.27 (6)

**Table B4.** Equivalent dose per photon fluence for the sensitive volume of the lens,  $H_s/\Phi$ , for the insensitive volume of the lens,  $H_i/\Phi$ , and for the entire lens of the eye,  $H_e/\Phi$ , for mono-energetic photons and PA exposure ( $180^\circ$ ) of the head and trunk. The values in brackets are the statistical one sigma standard uncertainties (absolute values of the most right digit, e.g. '0.00775 (20)' means ' $0.00775 \pm 0.00020$ '). The overall uncertainty is the geometrical sum of the statistical uncertainty and the non-statistical uncertainty which is estimated to be 2% (3.6% below 40 keV), see section 2.3.

Photon energy (MeV)	Equivalent dose per photon fluence (pSv cm <sup>2</sup> ) to the		
	sensitive volume $H_s/\Phi$	insensitive volume $H_i/\Phi$	entire lens $H_e/\Phi$
0.005	0 (-)	0 (-)	0 (-)
0.006	0 (-)	0 (-)	0 (-)
0.007	0 (-)	0 (-)	0 (-)
0.008	0 (-)	0 (-)	0 (-)
0.009	0 (-)	0 (-)	0 (-)
0.010	0 (-)	0 (-)	0 (-)
0.011	0 (-)	0 (-)	0 (-)
0.013	0 (-)	0 (-)	0 (-)
0.015	0 (-)	0 (-)	0 (-)
0.017	0 (-)	0 (-)	0 (-)
0.020	0.000 019 (19)	0.000 016 (9)	0.000 017 (8)
0.024	0.000 44 (10)	0.000 44 (5)	0.000 44 (5)
0.030	0.0042 (4)	0.004 90 (17)	0.004 78 (15)
0.040	0.0199 (9)	0.0202 (4)	0.0201 (4)
0.050	0.0327 (12)	0.0329 (5)	0.0328 (5)
0.060	0.0407 (13)	0.0420 (6)	0.0417 (6)
0.070	0.0462 (12)	0.0512 (7)	0.0504 (6)
0.080	0.0602 (17)	0.0588 (7)	0.0590 (7)
0.100	0.0752 (16)	0.0786 (8)	0.0780 (8)
0.120	0.099 (3)	0.1018 (10)	0.1013 (9)
0.150	0.137 (3)	0.1424 (12)	0.1415 (11)
0.200	0.222 (4)	0.2260 (17)	0.2253 (15)
0.240	0.288 (5)	0.300 (3)	0.2981 (20)
0.300	0.418 (7)	0.429 (3)	0.427 (3)
0.400	0.639 (9)	0.664 (5)	0.659 (5)
0.500	0.888 (12)	0.911 (7)	0.907 (6)
0.600	1.165 (15)	1.170 (8)	1.169 (7)
0.800	1.689 (20)	1.712 (11)	1.708 (10)
1.000	2.23 (3)	2.233 (14)	2.232 (13)
1.200	2.77 (3)	2.759 (17)	2.760 (15)
1.300	3.02 (3)	2.992 (18)	2.997 (16)
1.500	3.47 (4)	3.49 (3)	3.485 (18)
1.700	3.99 (4)	3.98 (3)	3.978 (20)
2.000	4.70 (4)	4.62 (3)	4.63 (3)
2.400	5.41 (4)	5.40 (3)	5.40 (3)
3.000	6.64 (5)	6.64 (4)	6.64 (3)

**Table B4.** (Continued.)

Photon energy (MeV)	Equivalent dose per photon fluence (pSv cm <sup>2</sup> ) to the		
	sensitive volume $H_s/\Phi$	insensitive volume $H_i/\Phi$	entire lens $H_e/\Phi$
4.000	8.45 (5)	8.46 (4)	8.46 (4)
5.000	10.03 (5)	10.18 (5)	10.15 (4)
6.000	11.62 (6)	11.64 (5)	11.64 (4)
8.000	14.66 (6)	14.82 (5)	14.79 (5)
10.000	17.56 (7)	17.87 (6)	17.82 (5)

**Table B5.** Equivalent dose per photon fluence for the sensitive volume of the lens,  $H_s/\Phi$ , for the insensitive volume of the lens,  $H_i/\Phi$ , and for the entire lens of the eye,  $H_e/\Phi$ , for mono-energetic photons and ROT exposure (0°–355°) of the head and trunk. The values in brackets are the statistical one sigma standard uncertainties (absolute values of the most right digit, e.g. '0. 007 75 (20)' means '0.007 75 ± 0.000 20'). The overall uncertainty is the geometrical sum of the statistical uncertainty and the non-statistical uncertainty which is estimated to be 2% (3.6% below 40 keV), see section 2.3.

Photon energy (MeV)	Equivalent dose per photon fluence (pSv cm <sup>2</sup> ) to the		
	sensitive volume $H_s/\Phi$	insensitive volume $H_i/\Phi$	entire lens $H_e/\Phi$
0.005	0.000 046 (8)	0.000 0023 (8)	0.000 0097 (15)
0.006	0.003 20 (7)	0.000 384 (11)	0.000 866 (15)
0.007	0.0368 (3)	0.007 59 (6)	0.012 60 (6)
0.008	0.1387 (6)	0.042 35 (13)	0.058 84 (14)
0.009	0.2961 (8)	0.1222 (3)	0.1520 (3)
0.010	0.4656 (11)	0.2377 (4)	0.2767 (4)
0.011	0.6055 (13)	0.3581 (5)	0.4005 (5)
0.013	0.7576 (16)	0.5436 (6)	0.5803 (6)
0.015	0.7892 (17)	0.6293 (7)	0.6566 (7)
0.017	0.7600 (18)	0.6446 (8)	0.6643 (7)
0.020	0.6702 (18)	0.6046 (8)	0.6159 (7)
0.024	0.5588 (18)	0.5279 (8)	0.5332 (8)
0.030	0.4468 (18)	0.4291 (8)	0.4322 (7)
0.040	0.3388 (17)	0.3349 (8)	0.3355 (7)
0.050	0.2954 (16)	0.2938 (7)	0.2941 (7)
0.060	0.2816 (15)	0.2851 (7)	0.2845 (7)
0.070	0.2903 (15)	0.2931 (7)	0.2926 (7)
0.080	0.3145 (15)	0.3143 (7)	0.3144 (7)
0.100	0.3769 (17)	0.3752 (8)	0.3755 (7)
0.120	0.4517 (19)	0.4506 (9)	0.4508 (8)
0.150	0.578 (3)	0.5802 (11)	0.5798 (10)
0.200	0.810 (4)	0.8094 (16)	0.8095 (14)

**Table B5.** (Continued.)

Photon energy (MeV)	Equivalent dose per photon fluence (pSv cm <sup>2</sup> ) to the		
	sensitive volume $H_s/\Phi$	insensitive volume $H_i/\Phi$	entire lens $H_e/\Phi$
0.240	1.010 (5)	1.0002 (20)	1.0019 (18)
0.300	1.274 (6)	1.285 (3)	1.283 (3)
0.400	1.744 (8)	1.756 (4)	1.754 (4)
0.500	2.216 (10)	2.217 (5)	2.217 (5)
0.600	2.615 (12)	2.642 (6)	2.637 (6)
0.800	3.476 (15)	3.451 (8)	3.455 (7)
1.000	4.206 (17)	4.202 (10)	4.203 (9)
1.200	4.844 (18)	4.869 (12)	4.865 (10)
1.300	5.104 (19)	5.196 (12)	5.180 (11)
1.500	5.59 (2)	5.784 (14)	5.751 (12)
1.700	5.93 (3)	6.258 (15)	6.201 (13)
2.000	6.35 (3)	6.833 (16)	6.750 (14)
2.400	6.84 (3)	7.393 (17)	7.299 (15)
3.000	7.22 (3)	7.985 (19)	7.854 (16)
4.000	7.92 (3)	8.748 (20)	8.607 (17)
5.000	8.61 (3)	9.50 (3)	9.351 (18)
6.000	9.29 (3)	10.14 (3)	9.997 (19)
8.000	10.69 (3)	11.55 (3)	11.40 (2)
10.000	11.85 (4)	12.88 (3)	12.70 (3)

**Table B6.** Equivalent dose per photon fluence for the sensitive volume of the lens,  $H_s/\Phi$ , for the insensitive volume of the lens,  $H_i/\Phi$ , and for the entire lens of the eye,  $H_e/\Phi$ , for mono-energetic photons incident at 45° on the head and trunk. The values in brackets are the statistical one sigma standard uncertainties (absolute values of the most right digit, e.g. '0.00775 (20)' means '0.00775 ± 0.00020'). The overall uncertainty is the geometrical sum of the statistical uncertainty and the non-statistical uncertainty which is estimated to be 2% (3.6% below 40 keV), see section 2.3.

Photon energy (MeV)	Equivalent dose per photon fluence (pSv cm <sup>2</sup> ) to the		
	sensitive volume $H_s/\Phi$	insensitive volume $H_i/\Phi$	entire lens $H_e/\Phi$
0.005	0.00012 (3)	0.000004 (3)	0.000023 (5)
0.006	0.0103 (3)	0.00125 (4)	0.00280 (6)
0.007	0.0954 (9)	0.02091 (18)	0.0337 (2)
0.008	0.3365 (17)	0.1110 (5)	0.1496 (5)
0.009	0.703 (3)	0.3095 (8)	0.3767 (8)
0.010	1.089 (4)	0.5857 (11)	0.6719 (11)
0.011	1.410 (4)	0.8737 (14)	0.9655 (14)
0.013	1.724 (5)	1.2772 (19)	1.3538 (18)
0.015	1.747 (6)	1.430 (3)	1.4841 (20)
0.017	1.619 (6)	1.413 (3)	1.448 (3)

**Table B6.** (Continued.)

Photon energy (MeV)	Equivalent dose per photon fluence (pSv cm <sup>2</sup> ) to the		
	sensitive volume $H_s/\Phi$	insensitive volume $H_i/\Phi$	entire lens $H_e/\Phi$
0.020	1.379 (6)	1.266 (3)	1.285 (3)
0.024	1.101 (5)	1.041 (3)	1.051 (3)
0.030	0.805 (5)	0.790 (3)	0.7929 (20)
0.040	0.577 (5)	0.5718 (20)	0.5727 (18)
0.050	0.476 (4)	0.4787 (19)	0.4782 (17)
0.060	0.449 (4)	0.4514 (18)	0.4511 (16)
0.070	0.447 (4)	0.4537 (17)	0.4526 (16)
0.080	0.475 (4)	0.4795 (18)	0.4788 (16)
0.100	0.564 (5)	0.5646 (19)	0.5645 (17)
0.120	0.662 (5)	0.667 (3)	0.6666 (19)
0.150	0.838 (6)	0.845 (3)	0.843 (3)
0.200	1.141 (8)	1.160 (4)	1.157 (4)
0.240	1.385 (10)	1.404 (5)	1.401 (5)
0.300	1.783 (13)	1.776 (7)	1.777 (6)
0.400	2.339 (18)	2.342 (9)	2.341 (8)
0.500	2.84 (3)	2.884 (12)	2.875 (10)
0.600	3.39 (3)	3.401 (14)	3.399 (12)
0.800	4.30 (4)	4.351 (18)	4.342 (16)
1.000	5.11 (4)	5.20 (3)	5.187 (20)
1.200	5.72 (4)	5.95 (3)	5.91 (3)
1.300	6.00 (5)	6.26 (3)	6.22 (3)
1.500	6.39 (5)	6.88 (3)	6.79 (3)
1.700	6.49 (5)	7.27 (4)	7.14 (3)
2.000	6.60 (5)	7.75 (4)	7.55 (3)
2.400	6.46 (5)	7.86 (4)	7.62 (4)
3.000	6.19 (5)	7.71 (4)	7.45 (4)
4.000	5.82 (5)	7.35 (4)	7.09 (4)
5.000	5.55 (4)	7.07 (4)	6.81 (3)
6.000	5.34 (4)	6.88 (4)	6.62 (3)
8.000	5.06 (4)	6.53 (4)	6.28 (3)
10.000	4.74 (4)	6.22 (4)	5.97 (3)

**Table B7.** Equivalent dose per photon fluence for the sensitive volume of the lens of the right and left eye for mono-energetic photons and LLAT exposure (90° from the left) of the head and trunk. The values in brackets are the statistical one sigma standard uncertainties (absolute values of the most right digit, e.g. '0. 007 75 (20)' means '0.007 75 ± 0.000 20'). The overall uncertainty is the geometrical sum of the statistical uncertainty and the non-statistical uncertainty which is estimated to be 2% (3.6% below 40 keV), see section 2.3.

Photon energy (MeV)	Equivalent dose per photon fluence (pSv cm <sup>2</sup> ) to the sensitive volume of the		
	left eye $H_{s,left}/\Phi$	right eye $H_{s,right}/\Phi$	Ratio $(H_{s,left}/\Phi)/(H_{s,right}/\Phi)$
0.005	0 (-)	0 (-)	-
0.006	0.000 12 (4)	0 (-)	-
0.007	0.0055 (3)	0 (-)	-
0.008	0.0395 (8)	0 (-)	-
0.009	0.1296 (16)	0 (-)	-
0.010	0.282 (3)	0 (-)	-
0.011	0.468 (4)	0 (-)	-
0.013	0.809 (5)	0.001 02 (17)	791 (125)
0.015	1.014 (6)	0.0035 (4)	287 (26)
0.017	1.090 (6)	0.0146 (7)	75 (4)
0.020	1.035 (7)	0.0485 (14)	21 (1)
0.024	0.907 (7)	0.109 (3)	8.3 (0.2)
0.030	0.708 (7)	0.159 (3)	4.5 (0.1)
0.040	0.530 (6)	0.192 (4)	2.8 (0.1)
0.050	0.439 (6)	0.196 (4)	2.24 (0.05)
0.060	0.427 (6)	0.206 (4)	2.08 (0.04)
0.070	0.423 (5)	0.222 (4)	1.90 (0.04)
0.080	0.452 (6)	0.252 (4)	1.79 (0.03)
0.100	0.540 (6)	0.307 (5)	1.76 (0.03)
0.120	0.640 (7)	0.374 (5)	1.71 (0.03)
0.150	0.791 (8)	0.493 (7)	1.61 (0.03)
0.200	1.121 (12)	0.730 (10)	1.54 (0.02)
0.240	1.392 (15)	0.909 (12)	1.53 (0.02)
0.300	1.746 (19)	1.178 (15)	1.48 (0.02)
0.400	2.36 (3)	1.70 (3)	1.39 (0.02)
0.500	2.85 (4)	2.16 (3)	1.32 (0.02)
0.600	3.33 (4)	2.58 (4)	1.29 (0.02)
0.800	4.33 (5)	3.46 (5)	1.25 (0.02)
1.000	5.08 (6)	4.32 (5)	1.17 (0.02)
1.200	5.89 (6)	4.95 (6)	1.19 (0.02)
1.300	6.26 (7)	5.18 (6)	1.21 (0.02)
1.500	6.76 (7)	5.81 (7)	1.16 (0.02)
1.700	7.14 (7)	6.49 (7)	1.10 (0.02)
2.000	7.72 (8)	7.17 (7)	1.08 (0.01)
2.400	8.27 (8)	8.14 (8)	1.02 (0.01)
3.000	8.65 (9)	9.20 (9)	0.94 (0.01)
4.000	8.83 (9)	10.72 (10)	0.82 (0.01)
5.000	8.66 (9)	12.38 (11)	0.70 (0.01)

**Table B7.** (Continued.)

Photon energy (MeV)	Equivalent dose per photon fluence (pSv cm <sup>2</sup> ) to the sensitive volume of the		
	left eye $H_{s,left}/\Phi$	right eye $H_{s,right}/\Phi$	Ratio $(H_{s,left}/\Phi)/(H_{s,right}/\Phi)$
6.000	8.69 (9)	13.70 (11)	0.63 (0.01)
8.000	8.29 (9)	16.81 (13)	0.49 (0.01)
10.000	7.92 (9)	18.99 (14)	0.42 (0.01)

## References

- Behrens R, Dietze G and Zankl M 2009 Dose conversion coefficients for electron exposure of the human eye lens *Phys. Med. Biol.* **54** 4069–87 (2010 *Phys. Med. Biol.* **55** 3937–45 corrigendum)
- Behrens R and Dietze G 2010 Monitoring the eye lens: which dose quantity is adequate? *Phys. Med. Biol.* **55** 4047–62
- Behrens R 2010 Inconsistencies in egsp (the EGSnrc C++ class library), and in the SLAB module of BEAMnrc *Phys. Med. Biol.* **55** L33–6 (2010 *Phys. Med. Biol.* **55** 6573–4 corrigendum)
- Berger M J and Hubbell J H 1987 XCOM: photon cross sections on a personal computer *Report NBSIR87-3597* (Gaithersburg, MD: National Institute of Technology)
- Bouchet L G, Bolch W E, Weber D A, Atkins H L and Poston J W Sr 1999 MIRD Pamphlet No. 15: radionuclide S values in a revised dosimetric model of the adult head and brain *J. Nucl. Med.* **40** 62S–101S
- Charles M W and Brown N 1975 Dimensions of the human eye relevant to radiation protection *Phys. Med. Biol.* **20** 202–18
- Chodick G *et al* 2008 Risk of cataract after exposure to low doses of ionizing radiation: a 20-year prospective cohort study among US radiologic technologists *Am. J. Epidemiol.* **168** 620–31
- Daures J, Gouriou J and Bordy J-M 2009 Conversion coefficients from air kerma to personal dose equivalent  $H_p(3)$  for eye-lens dosimetry *CEA-R-6235* (Gif-sur-Yvette: CEA)
- Hubbell J H and Seltzer S M 1995 Tables of x-ray mass attenuation coefficients and mass energy-absorption coefficients 1 keV to 20 MeV for elements  $Z = 1$  to 92 and 48 additional substances of dosimetric interest *Report NISTIR 5632* <http://physics.nist.gov/PhysRefData/XrayMassCoef/cover.html>
- International Commission on Radiological Protection (ICRP) 1996 Conversion coefficients for use in radiological protection against external radiation *ICRP Publication 74* (Oxford: Pergamon)
- International Commission on Radiological Protection (ICRP) 2003 Basic anatomical and physiological data for use in radiological protection: reference values *ICRP Publication 89* (Oxford: Pergamon)
- International Commission on Radiological Protection (ICRP) 2007 The 2007 recommendations of the International Commission on Radiological Protection *ICRP Publication 103* (Amsterdam: Elsevier)
- Kawrakow I 2005 egsp: the EGSnrc C++ class library *NRCC Report PIRS-899* <http://irs.inms.nrc.ca/software/egsnrc/documentation/pirs898/index.html>
- Kawrakow I and Rogers D W O 2006 The EGSnrc code system: Monte Carlo simulation of electron and photon transport *NRCC Report PIRS-701* <http://irs.inms.nrc.ca/software/egsnrc/documentation/pirs701/index.html>
- Kramer R, Zankl M, Williams G and Drexler G 1982 The calculation of dose from external photon exposures using reference human phantoms and Monte-Carlo methods. Part I. The male (ADAM) and female (EVA) adult mathematical phantoms *GSF Bericht S-885* (Neuherberg: GSF)
- Mariotti F and Gualdrini G 2009 A new Monte Carlo approach to define the operational quantity  $H_p(3)$  *RT/2009/1/BAS* (Bologna: ENEA)
- Schlattl H, Zankl M and Petoussi-Hens N 2007 Organ dose conversion coefficients for voxel models of the reference male and female from idealized photon exposures *Phys. Med. Biol.* **52** 2123–45
- Worgul B V *et al* 2007 Cataracts among chernobyl clean-up workers: implications regarding permissible eye exposures *Radiat. Res.* **167** 223–43